

Crystallization and Structure Determination of Bovine Profilin at 2.0 Å Resolution

Eila S. Cedergren-Zeppezauer¹†, Nalin C. W. Goonesekere²
Michael D. Rozycki², James C. Myslik², Zbigniew Dauter³
Uno Lindberg¹ and Clarence E. Schutt²‡

¹*Department of Zoological Cell Biology, WGI, Arrhenius Laboratories for Natural Sciences
Stockholm University, S-10691 Stockholm, Sweden*

²*Department of Chemistry, Henry H. Hoyt Laboratory
Princeton University, Princeton, NJ 08544, U.S.A.*

³*European Molecular Biology Laboratory (EMBL), DESY
Notkestraße 85, D-2000 Hamburg 52, Germany*

Profilin regulates the behavior of the eukaryotic microfilament system through its interaction with non-filamentous actin. It also binds several ligands, including poly(L-proline) and the membrane phospholipid phosphatidylinositol 4,5-bisphosphate (PtdIns(4,5)P₂). Bovine profilin crystals (space group *C*2; $a=69.15$ Å, $b=34.59$ Å, $c=52.49$ Å; $\alpha=\gamma=90^\circ$, $\beta=92.56^\circ$) were grown from a mixture of poly(ethylene glycol) 400 and ammonium sulfate. X-ray diffraction data were collected on an imaging plate scanner at the DORIS storage ring (DESY, Hamburg), and were phased by molecular replacement, using a search model derived from the 2.55 Å structure of profilin complexed to β -actin. The refined model of bovine profilin has a crystallographic *R*-factor of 16.5% in the resolution range 6.0 to 2.0 Å and includes 128 water molecules, several of which form hydrogen bonds to stabilize unconventional turns.

The structure of free bovine profilin is similar to that of bovine profilin complexed to β -actin, and C α atoms from the two structures superimpose with an r.m.s. deviation of 1.25 Å. This value is reduced to 0.51 Å by omitting Ala1 and the N-terminal acetyl group, which lie at a profilin-actin interface in crystals of the complex. These residues display a strained conformation in crystalline profilin-actin but may allow the formation of a hydrogen bond between the *N*-acetyl carbonyl group of profilin and the phenol hydroxyl group of Tyr188 in actin. Several other actin-binding residues of profilin show different side-chain rotamer conformations in the two structures. The polypeptide fold of bovine profilin is generally similar to those observed by NMR for profilin from other sources, although the N terminus of *Acanthamoeba* profilin isoform I lies in a distorted helix and the C-terminal helix is less tilted with respect to the strands in the central β -pleated sheet than is observed in bovine profilin.

The majority of the aromatic residues in profilin are exposed to solvent and lie in either of two hydrophobic patches, neither of which takes part in an interface with actin. One of these patches is required for binding poly(L-proline) and contains an aromatic cluster comprising the highly conserved residues Trp3, Tyr6, Trp31 and Tyr139. In forming this cluster, Trp31 adopts a sterically strained rotamer conformation. This patch is surrounded by basic residues at the carboxyl terminus of profilin and at the turns connecting strand 1 to strand 2 and strand 6 to strand 7, providing a plausible binding site for micellar PtdIns(4,5)P₂.

Keywords: actin; crystal; molecular replacement; profilin;
protein structure

† Present address: Department of Structural Chemistry, (FOS), Arrhenius Laboratories for Natural Sciences, Stockholm University, S-10691 Stockholm, Sweden.

‡ Author to whom all correspondence should be addressed.

1. Introduction

Profilins are small (13 to 15 kDa) actin-binding proteins found abundantly in organisms ranging from yeast to humans (for a recent review, see Machesky & Pollard, 1993). Profilin was first isolated from calf spleen as a crystallizable 1:1 complex with actin which inhibited the activity of deoxyribonuclease I (Lindberg, 1966; Carlsson *et al.*, 1976). *In vitro*, profilin forms a stable complex with actin (profilin-actin), which led to the early view that profilin is an actin monomer-sequestering protein (Carlsson *et al.*, 1977). This view was supported by observations in *Thyone* sperm that high concentrations of monomeric actin stored as profilin-actin are capable of rapid filament assembly (Tilney *et al.*, 1983).

Recent observations require a reconsideration of the notion that profilin is merely a cellular actin-sequestering protein. First, other actin-binding factors, such as thymosin β_4 (Safer *et al.*, 1990), have been identified as predominant intracellular actin-sequestering agents (Weber *et al.*, 1992; Carlier *et al.*, 1993). At the same time, evidence has accumulated that profilin may actually facilitate actin filament assembly under certain conditions. Filament barbed ends are selectively elongated *in vitro* when either *Limulus* acrosomal false discharges are used as nuclei (Pring *et al.*, 1992) or when assembly takes place in the presence of thymosin β_4 (Pantaloni & Carlier, 1993). In addition, over-expression of profilin leads to a net stabilization of actin filaments in Chinese Hamster Ovary cells (Finkel *et al.*, 1994). Finally, the crystal structure of profilin- β -actin at 2.55 Å resolution (Schutt *et al.*, 1993) shows that profilin forms two extensive interfaces with actin (Schutt *et al.*, 1989, 1993), providing the first structural evidence that profilin could bind to oligomeric assemblies of actin.

Profilin also appears to be an important link between phosphoinositide lipid-based signal transduction and the eukaryotic microfilament system. Specific binding of profilin to the anionic phospholipid phosphatidylinositol 4,5-bisphosphate (PtdIns(4,5)P₂)† dissociates the profilin-actin complex (Lassing & Lindberg, 1985), and profilin protects PtdIns(4,5)P₂ from hydrolysis by phospholipase C- γ 1 (Goldschmidt-Clermont *et al.*, 1990). Hydrolysis of PtdIns(4,5)P₂ occurs when cells are stimulated by signalling agents such as growth factors, hormones, or neurotransmitters and yields the secondary messengers diacyl glycerol and inositol trisphosphate (Berridge, 1987, 1993; Nishizuka, 1992). The inhibitory effect of profilin on the hydrolysis of PtdIns(4,5)P₂ by phospholipase C- γ 1 can be overcome *in vitro* by phosphorylation of phospholipase C- γ 1 via the tyrosine kinase activity of the EGF receptor (Goldschmidt-Clermont *et al.*, 1991). Several other actin-binding proteins interact with PtdIns(4,5)P₂ to regulate actin assembly,

including gelsolin (Janmey & Stossel, 1987; Yu *et al.*, 1992), villin (Janmey *et al.*, 1992) and severin (Eichinger & Schleicher, 1992).

An indication that profilin may play additional, as yet uncharacterized, roles in cell signalling came from the observation that six highly conserved hydrophobic residues form a surface patch distinct from, but immediately adjacent to, the two actin-binding surfaces of bovine profilin (Schutt *et al.*, 1993). Mutagenesis of Trp3 and His133 established that the specificity of human profilin for poly(L-proline) localizes to this patch (Björkegren *et al.*, 1993), a result also found by NMR for human (Metzler *et al.*, 1994) and *Acanthamoeba* (Archer *et al.*, 1994) profilins. Thus, profilin shares with Src homology 3 (SH3) domains the characteristic of binding proline-enriched peptides to predominantly aromatic surface patches, suggesting that the specificity of profilin for poly(L-proline) mimics a still-undiscovered ligand-binding function in the cell (Schutt *et al.*, 1993; Rozycki *et al.*, 1994). In fact, the polypeptide fold of profilin contains an SH3-like fold (Schutt *et al.*, 1993), although it is not coincident with the conserved hydrophobic patch.

Furthermore, profilin is a prominent allergenic component in pollens from birch, timothy grass and mugwort, eliciting type 1 allergic responses such as asthma, conjunctivitis and rhinitis (Valenta *et al.*, 1991, 1992). Immunoglobulin E present in sera of allergic patients can cross-react with profilins from a variety of distantly related plants, suggesting that these plant profilins contain a common epitope (Valenta *et al.*, 1992). This epitope appears to be shared with human profilin, as the addition of human profilin to basophils cultured from patients allergic to plant profilin also stimulates the release of histamine (Valenta *et al.*, 1991). Since the human and bovine isoforms of profilin are closely related, the high resolution structure of bovine profilin should aid in the identification of the allergenic epitopes in the plant profilins.

Thus, profilin appears to lie at the focus of a complex connection between cellular signalling and the regulation of actin filament assembly. Although the solution NMR structures have been described for human and *Acanthamoeba* profilin (Metzler *et al.*, 1993; Vinson *et al.*, 1993) and the interfaces between bovine profilin and actin have been described by X-ray crystallography (Schutt *et al.*, 1993), a description of the structural changes in profilin in forming its contacts with actin requires direct comparison of the free and actin-bound structures of profilin from one source. In addition, a high-resolution description of surface residues in profilin will be important for interpreting eventual crystal structures of profilin complexed to various ligands. To these ends, we describe here the structure of free bovine profilin to a resolution of 2.0 Å.

2. Materials and Methods

(a) Crystallization

Bovine profilin was obtained as described (Rozycki *et al.*, 1991) from spleen of thymic tissue. Purified protein

† Abbreviations used: PtdIns(4,5)P₂, phosphatidylinositol 4,5-bisphosphate; SH3, Src homology 3; PEG 400, poly(ethylene glycol) 400; F-actin, filamentous actin.

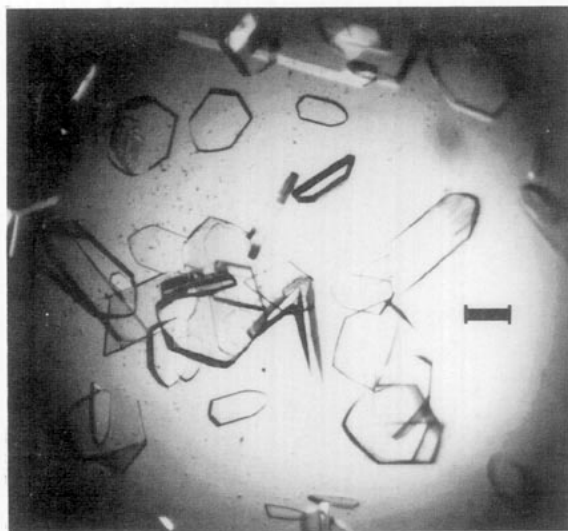


Figure 1. Light micrograph of calf spleen profilin crystals. Plate thickness usually does not exceed 50 μm . The bar corresponds to 0.5 mm.

was stored as a precipitate in 80% saturated ammonium sulfate at 4°C and neutral pH. Prior to crystallization, precipitated protein was dissolved in 5.0 mM phosphate at pH 7.6 to a concentration of 50 mg profilin/ml and centrifuged. This stock solution was then used either directly or after dialysis in glass capillaries (Zeppezauer *et al.*, 1968) for adjustment of pH and ionic strength.

A preliminary screen using the sparse matrix method (Jancarik & Kim, 1991) covered 50 different crystallization conditions. Crystals were observed in the pH range 5.8 to 8.5 using a variety of precipitating agents. Of 6 distinct crystal habits observed, 3 were shown by SDS gel electrophoresis (Laemmli, 1970) to contain profilin. Profilin purified from either spleen or thymus tissue formed crystals in the temperature range from 4°C to room temperature. Crystals suitable for crystallographic analysis were obtained in a mixture of poly(ethylene glycol) 400 (PEG 400) and ammonium sulfate.

Conditions were then optimized to grow crystals large enough for X-ray data collection using the sitting drop method. A plastic micro-bridge (Crystal Microsystems, K. Harlos, Oxford, U.K.) was placed into each well of a Linbro culture plate followed by 1 ml of outer solution (1.5% PEG 400, 2.0 M ammonium sulfate, 10 mM β -mercaptoethanol). Profilin stock was diluted with 0.1 M Hepes (pH 7.5 at 4°C), giving a profilin concentration of 14 mg/ml. This solution was placed on the micro-bridge and mixed with an equal volume of outer solution. The well was sealed and crystals were grown at 4°C over a period of 2 to 3 weeks. Crystals grown under these conditions melt at room temperature. They belong to space group $C2$ with $a=69.15$ Å, $b=34.59$ Å, $c=52.49$ Å; $\alpha=\gamma=90^\circ$, $\beta=92.56^\circ$. Representative crystals are shown in Figure 1.

(b) Data Collection

X-ray data were collected on the X31 EMBL beamline located on the DORIS storage ring (DESY, Hamburg) operating at 5.25 GeV in multi-bunch mode. A wavelength of 1.008 Å and a square aperture of 0.35 mm \times 0.35 mm were used. The temperature along the capillary wall was maintained at 4°C by a stream of cold air. X-ray

intensities were collected on an imaging plate scanner constructed at EMBL (J. Hendrix & A. Lentfer, unpublished results) using the rotation method developed for photographic film. Oscillation ranges were set at the angle subtended by the crystal cell dimensions in order to avoid spatial overlap of recorded reflections (Arndt & Wonacott, 1977). All datasets were collected from a single crystal of dimensions 0.30 mm \times 0.15 mm \times 0.05 mm in 2 180° sweeps at 2.0 and 2.6 Å resolution, respectively. The low resolution pass was needed to recover reflections saturated during the longer collection times used in the high resolution pass. Intensities were evaluated using the profile-fitting option implemented in a modification of the MOSFLM (Leslie *et al.*, 1986) program package and were merged and averaged using the CCP4 program suite (Daresbury Laboratory).

(c) Phasing

X-ray amplitudes were phased by molecular replacement, using as a search object a 2.55 Å resolution model of bovine profilin obtained at an intermediate stage of its refinement in a complex with actin (this model was similar to the profilin model described by Schutt *et al.* (1993) except that it included only residues Cys16 through Arg136). All rotational and translational searches were carried out with X-PLOR (Brünger, 1992) in the resolution range 6.0 to 3.0 Å. The 3000 highest peaks in the Patterson map corresponding to difference vectors of lengths between 5.0 and 20.0 Å were chosen for the rotation search. Correct rotational parameters were found at the maximum of the rotation function map at a peak height of 3.1 (7.4σ above the mean). The next highest peak in the map was at 2.5. The 34 highest peaks of the rotation function calculations were used in a Patterson correlation refinement (Brünger, 1990), and correlation coefficients of 0.244 and 0.168 were obtained for the 2 best solutions. A translation search using the best solution gave a maximum at a peak height of 0.41 (9.25σ above the mean), and rigid body refinement of this rotational/translation solution produced a starting model with an R -factor of 47.6%. Atomic temperature factors for this starting model were set to 20 Å².

At this point, residues 1 to 15 and 137 to 139 were added to the starting model by fitting to a $2F_o - F_c$ map using the molecular graphics program FRODO (Jones, 1978). The conformation of the polypeptide chain for these residues was almost identical to that of profilin bound to β -actin, except for the positions of Ala1 and the N -acetyl group. The now-complete model was subjected to conjugate gradient minimization and simulated annealing refinement as implemented in X-PLOR (Brünger, 1992), using bond length and angle parameters derived from the Cambridge Data Base of model structures (Engh & Huber, 1991). The temperature range chosen for simulated annealing was between 3000 K and 300 K and the resolution range was 7.0 to 3.0 Å. The R -factor at the end of this refinement was 22.0%. The resolution of the refinement was gradually extended to 2.0 Å in several steps, each involving a cycle of map generation, model evaluation and simulated annealing refinement. With the addition of each resolution shell, the R -factor increased somewhat, finishing at 23.0% after a grouped temperature factor refinement at 6.0 to 2.0 Å resolution.

Next, side-chain orientations were evaluated using 'omit maps' generated from protocols implemented in X-PLOR (Brünger, 1992) and were adjusted as necessary using FRODO. After examination of $2F_o - F_c$ and $F_o - F_c$

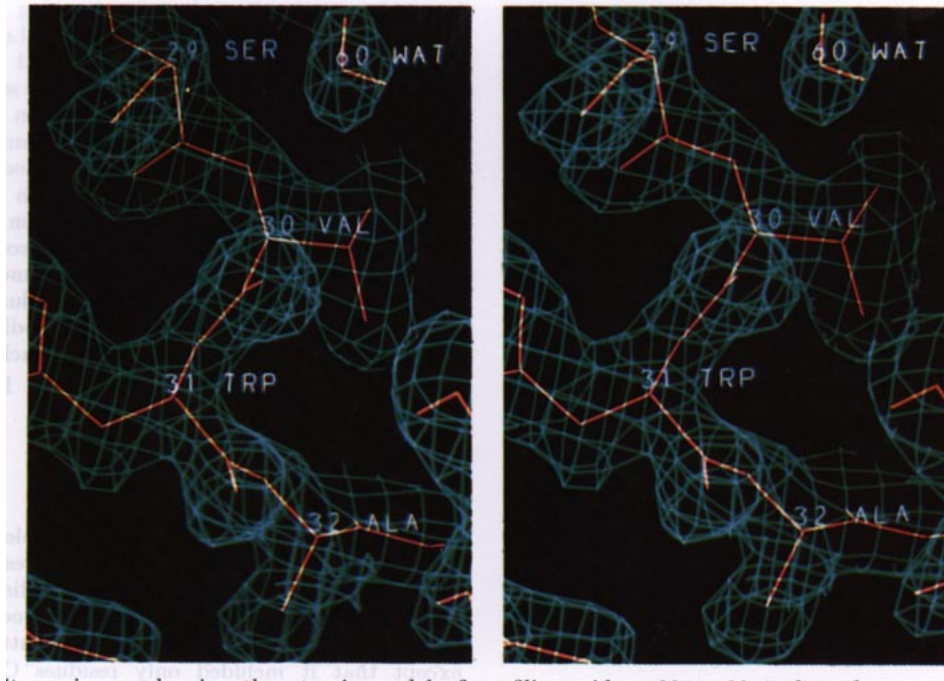


Figure 2. Stereo image showing the atomic model of profilin residues 29 to 32 (red) and accompanying $2F_o - F_c$ electron density (green cage) calculated from the final refined model. Water molecule 60 hydrogen bonds to the amide nitrogen (and associated hydrogen atom) of Val30. Map contouring level is 1.0σ . Figure made using FRODO (Jones, 1978).

electron density maps, water molecules were placed so that each had at least 1 hydrogen bonding interaction either with profilin or with another water molecule. This model was subjected to simulated annealing and temperature-factor refinement and water molecules with tempera-

ture factors greater than 50 \AA^2 were omitted. The final model contained 128 water molecules and the crystallographic R -factor for data between 6.0 and 2.0 Å was 16.5%.

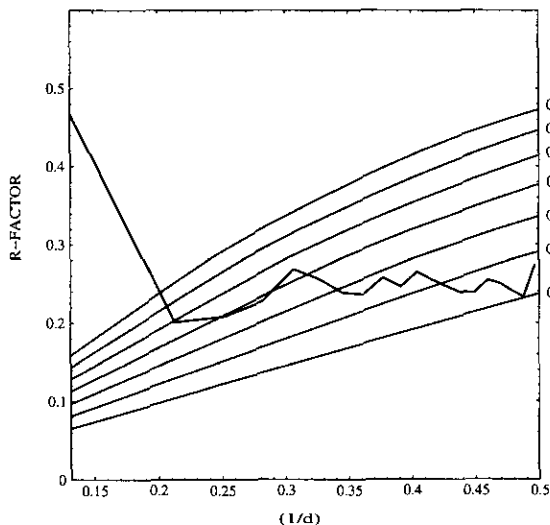


Figure 3. Luzatti plot of crystallographic R -factor as a function of resolution ($1/d$) for 2.0 Å resolution refinement of bovine profilin and crystallographically ordered water molecules. Curves pass through the origin and represent theoretically calculated (Luzatti, 1952) co-ordinate errors of 0.20, 0.25, ..., 0.50 Å. The observed R -factor plot gives an estimated co-ordinate error between 0.25 and 0.30 Å. Normally, observed R -factors stabilize between 2 theoretical lines at medium to high resolution (increasing $1/d$). Thus, the profilin-water model appears to have better-than-expected R -factors at high resolution.

3. Results

(a) Quality of the final model

Statistics for the 2.0 Å refinement of bovine profilin are given in Table 1 and a representative portion of $2F_o - F_c$ electron density calculated from the final refined model is shown in Figure 2. The

Table 1
Data processing and refinement statistics

Resolution (Å)	Reflections		R -factor (%)	$R_{cum}\S$ (%)
	Unique†	Completeness‡ (%)		
6.00–4.78	308	100.0	19.9	19.9
4.78–3.94	501	100.0	11.3	14.9
3.94–3.43	588	100.0	13.3	13.7
3.43–3.08	661	100.0	15.2	14.0
3.08–2.81	727	100.0	15.8	14.4
2.81–2.61	779	100.0	17.8	14.9
2.61–2.44	825	100.0	18.1	15.4
2.44–2.31	872	100.0	18.2	15.7
2.31–2.19	954	99.8	18.6	16.0
2.19–2.09	986	99.5	19.8	16.3
2.09–2.00	697	68.0	19.5	16.5

† $R_{merge} = \sum |I - \langle I \rangle| / \sum I = 6.6\%$ for 29,297 experimentally measured reflections yielding 8239 unique reflections. I is the intensity of a given reflection and $\langle I \rangle$ is the mean intensity of equivalent reflections.

‡ $|F| > 3\sigma|F|$.

§ Cumulative R -factor.

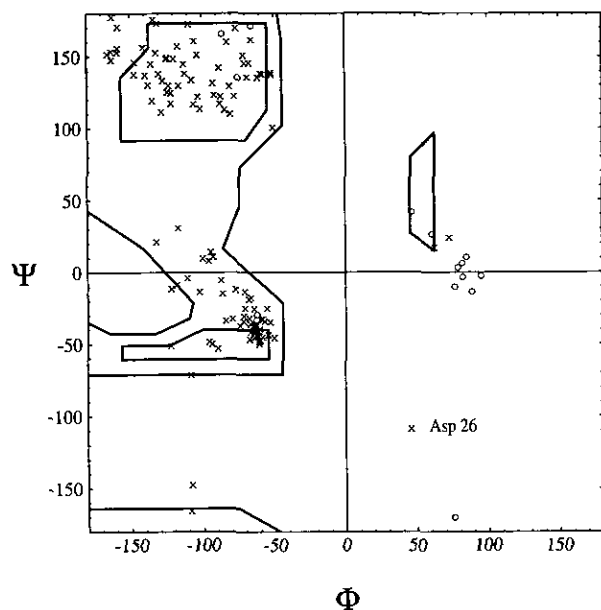


Figure 4. Ramachandran plot of ϕ versus ψ angles in bovine profilin refined at 2.0 Å resolution. Positions of non-glycine and glycine residues are indicated with crosses and open circles, respectively. Asp26 takes the $i+1$ position of a γ -turn (Baker & Hubbard, 1984) that connects strands 1 and 2 (see Figure 9(a)).

structure has tight stereochemical restraints: r.m.s. deviations in geometry are 0.011 Å for bond lengths, 1.54° for bond angles, 24.99° for dihedral angles and 1.39° for improper angles. An upper estimate of the overall error in the positions of atomic co-ordinates, derived by plotting the R -factor as a function of resolution (Luzatti, 1952), is shown in Figure 3. Compared to theoretical curves based on random positional errors, the estimated r.m.s. error in atomic co-ordinates of the refined model is 0.20 to 0.25 Å. The (ϕ, ψ) values of all non-glycine residues fall within or near energetically allowed regions of a Ramachandran plot, shown in Figure 4. The only exception is Asp26, which lies in a γ -turn (see

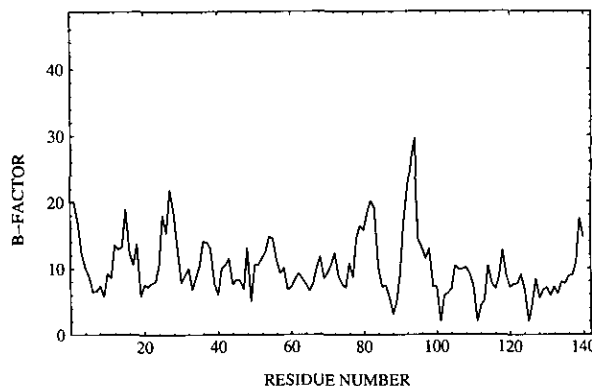


Figure 5. Plot of grouped temperature factors for main-chain atoms (O, N, C, C α) by residue for 2.0 Å refinement of bovine profilin. Solvent molecules are not included. The mean atomic temperature factor for protein and solvent is 10.8 Å². The highest peak corresponds to the loop connecting Lys90 through Pro96, which forms a solitary protrusion.

Figure 9). Average grouped temperature factors for the model are 10.8 Å² for main-chain atoms (Figure 5), 15.8 Å² for side-chain atoms and 29.0 Å² for water molecules. The electron density of omit maps provided excellent fit for most residues. Residues in the loop connecting Lys90 with Pro96 have the weakest electron density and the highest temperature factors in the structure.

(b) Structure of profilin

The polypeptide fold of free bovine profilin is shown in Figure 6 and secondary structural elements are summarized in Table 2. Profilin contains a central six-stranded antiparallel β -sheet, with N and C-terminal helices (helix 1 and helix 4, respectively) adjacent to each other on one side of the sheet. Two small helices (helix 2 and helix 3) and a β -hairpin lie on the opposite surface of the sheet. Residues Trp31 and Ile73 lie at β -bulges, which direct (Richardson & Richardson, 1989) strands 2

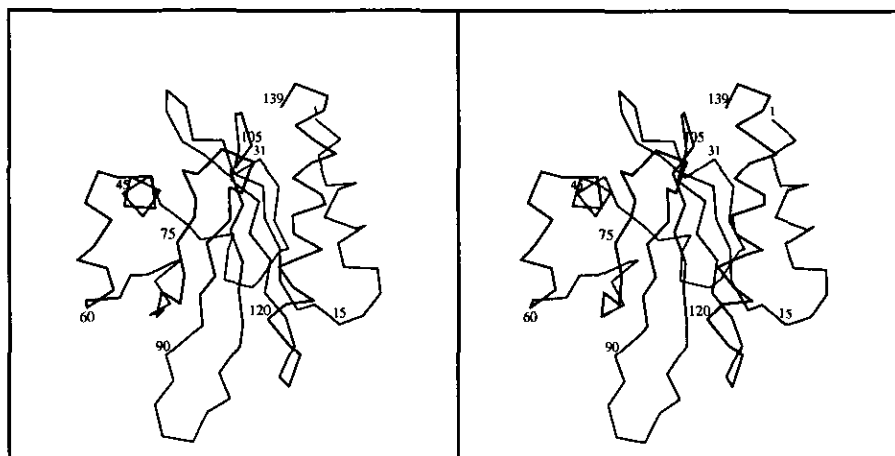


Figure 6. Structure of bovine profilin refined to 2.0 Å resolution. The polypeptide fold is depicted by a stereo plot of C α -atoms. Residues are labelled in increments of 15 residues. Secondary structure elements are given in Table 2. Figure made using MOLSCRIPT (Kraulis, 1991).

Table 2
Secondary structural elements

Helices	Reverse turns†
(1) 33–12	(1) 25–27 γ ‡
(2) 43–52	(2) 34–37 II
(3) 56–62	(3) 32–42 I
(4) 119–137	(4) 65–68 I'
	(5) 76–79 I
β -Strands	(6) 79–82 II
(1) 18–24	(7) 92–95 I'
(2) 28–33§	(8) 105–108 I
(3) 62–64	(9) 115–118 II
(4) 69–75§	
(5) 83–89	
(6) 98–104	
(7) 109–114	

† Turns labeled according to Venkatachalam (1968) and Wilmot & Thornton (1988).

‡ γ -turn, defined by Baker & Hubbard (1984).

§ Residues Trp31 and Ile73 adopt β -bulge conformation.

and 4 away from the sheet. In fact, the topology of profilin could also be described as a single, seven-stranded β -sheet. In this case, the β -hairpin arising from the β -bulge at Ile73 can be considered a continuation of the central sheet.

The main hydrophobic core of profilin lies on the face of the central sheet bounded by helices 2 and 3 and strands 3 and 4 (see section (d), below). Strands 1, 6 and 7 of the central β -sheet are at the interior of the molecule and are mostly buried from solvent. Two reverse turns (5 and 6 in Table 2) occur in succession between residues Ser76 and Glu82. Turn 5 directs the side-chains of Leu77 and Leu78 towards the main hydrophobic core of profilin, capping it between helix 2 and strand 4. Turn 6 connects strands 4 and 5. Tight turns connect the remaining strands within the β -sheet, except for a γ -turn between strands 1 and 2. Hydrogen bonding interactions involving elements of secondary structure in the refined model are given in Table 3.

Profilin resembles actin-binding domains in gelsolin (segment 1) (McLaughlin *et al.*, 1993) and villin (14T) (Markus *et al.*, 1994). All three structures are approximately the same size and are built around a central β -sheet with N and C-terminal helices lying on one side of the sheet and a mixture of small helices and β -strands lying against the other side. However, the polypeptide folds of gelsolin segment 1 and villin 14T are completely different from the fold of profilin (Rozycki *et al.*, 1994). Somewhat surprisingly, the folding motif comprising strands 3 through 6 of bovine profilin is similar to several recently elucidated (Noble *et al.*, 1993) Src homology 3 (SH3) domains (Schutt *et al.*, 1993).

(c) Comparison of free profilin with profilin bound to actin

C α atoms from free bovine profilin superimpose onto those of profilin bound to β -actin (Schutt *et al.*, 1993) with an overall r.m.s. deviation of 1.25 Å. The

Table 3
Hydrogen bonding of secondary structural elements in profilin

Donor atom	Acceptor atom	Bond length (Å)	Bond angle (°)†	ϕ (°)	ψ (°)
A. Alpha helices					
Helix 1					
Trp3 N	Ac O	2.8	18	-68	-20
Ala5 N	Gly2 O	3.2	15	-68	-32
Tyr6	Trp3 O	3.3	39	-68	-38
Asp8 N	Asn4 O	3.0	16	-55	-44
Asn9 N	Ala5 O	3.2	23	-61	-50
Leu10 N	Tyr6 O	3.1	12	-59	-33
Met11 N	Ile7 O	2.9	30	-87	-6
Met11 N	Asp8 O	3.3	59	-87	-6
Ala12 N	Asn9 O	3.0	25	-64	-38
Helix 2					
Thr43 N	Glu46 O ²	3.1	24	-105	160
Glu46 N	Thr43 O ¹	3.3	23	-64	-34
Val47 N	Thr43 O	3.1	24	-67	-41
Gly48 N	Pro44 O	2.9	34	-63	-33
Ile49 N	Ala45 O	3.3	30	-74	-38
Ile49 N	Glu46 O	3.3	56	-74	-38
Leu50 N	Glu46 O	3.2	26	-63	-41
Val51 N	Val47 O	3.2	20	-100	9
Gly52 N	Ile49 O	3.4	21	-66	171
Helix 3					
Ser56 N	Asp54 O ²	3.0	21	-123	51
Ser57 N	Asp54 O ²	3.0	12	-53	-35
Phe59 N	Ser56 O	2.9	28	-71	-25
Val60 N	Ser57 O	2.9	39	-96	-48
Asn61 N	Ser57 O	2.8	4	-86	-15
Helix 4					
Met122 N	His119 O	3.3	50	-67	-42
Ile123 N	His119 O	3.4	18	-65	-43
Asn124 N	Gly120 O	2.8	27	-61	-48
Asn124 N ²	Asp86 O ²	2.8	21	-61	-48
Asn124 N ²	Thr84 O ¹	3.3	25	-61	-48
Lys125 N	Gly121 O	3.0	17	-72	-31
Lys126 N	Met122 O	3.2	23	-68	-47
Cys127 N	Ile123 O	3.0	14	-61	-45
Tyr128 N	Asn124 O	2.9	18	-59	-46
Asp129 N	Lys125 O	2.9	18	-65	-37
Met130 N	Lys126 O	3.0	18	-64	-45
Ala131 N	Cys127 O	3.0	10	-60	-40
Ser132 N	Tyr128 O	2.8	27	-65	-38
Ser132 O ⁷	Tyr28 O	3.0	28	-65	-38
His133 N	Asp129 O	3.0	27	-60	-48
Leu134 N	Met130 O	3.0	18	-64	-41
Arg135 N	Ala131 O	2.9	21	-61	-42
Arg136 N	Ser132 O	3.0	20	-64	-26
Ser137 N	His133 O	3.4	45	-94	14
Ser137 N	Leu134 O	3.0	48	-94	14
Gln138 N	Arg135 O	3.0	25	72	24
Tyr139 N	Leu134 O	2.9	19		
B. Anti-parallel sheet					
Asp18 N	Met113 O	3.4	32	-158	155
Ala19 N	Asp18 O ¹	2.9	49	-166	151
Ala20 N	Leu111 O	3.0	30	-159	153
Ile21 N	Ala32 O	2.9	11	-122	117
Val22 N	Leu109 O	2.8	13	-124	125
Gly23 N	Ser29 O	2.9	36	-75	135
Tyr24 N	Lys107 O	3.1	24	-111	-4
Ser29 N	Gly23 O	3.4	31	-163	153
Val30 N	Wat60 OH2	3.0	15	-78	122
Trp31 N	Ile21 O	2.8	31	-84	-34
Ala32 N	Ile21 O	3.3	27	-163	147
Gly62 N	Phe58 O	2.8	41	76	-170
Leu63 N	Cys70 O	3.0	23	-158	171

Table 3 (continued)

Donor atom	Acceptor atom	Bond length (Å)	Bond angle (°)†	ϕ (°)	ψ (°)
<i>B. Anti-parallel sheet</i>					
Thr64 N	Wat68 OH2	3.1	15	-124	149
Lys69 N ^c	Leu63 O	3.4	53	-68	135
Lys69 N	Wat47 OH2	2.8	18	-68	135
Cys70 N	Leu63 O	2.7	38	-140	156
Ser71 N	Arg88 O	2.7	18	-113	145
Val72 N	Wat34 OH2	2.9	14	-92	123
Ile73 N	Asp86 O	2.7	28	-90	-53
Arg74 N	Asp86 O	3.3	22	-147	145
Phe83 N	Gln79 O	2.9	37	63	17
Met85 N	Val102 O	2.9	39	-137	130
Asp86 N	Arg74 O	2.9	22	-107	133
Leu87 N	Ile100 O	2.8	12	-134	176
Arg88 N	Ser71 O	3.0	32	-147	137
Thr89 N	Phe98 O	3.0	18	-71	150
Phe98 N	Thr89 O ¹	2.9	17	-125	148
Asn99 N	Wat36	2.9	11	-88	142
Ile100 N	Leu87 O	3.0	10	-135	145
Thr101 N	Leu112 O	3.0	26	-130	138
Val102 N	Met85 O	2.9	13	-116	130
Thr103 N	Val110 O	2.9	20	-127	133
Met104 N	Phe83 O	2.9	23	-92	131
Leu109 N	Val22 O	2.8	37	-122	124
Val110 N	Thr103 O	2.9	12	-106	117
Leu111 N	Ala20 O	2.9	11	-112	138
Leu112 N	Thr101 N	3.0	28	-140	137
Met113 N	Asp18 O	3.0	16	-123	130
Gly114 N	Asn99 O	2.9	11	-86	166

† Donor-H-acceptor angle; a linear hydrogen bond has an angle of zero.

only significant deviation in the folds of the two structures occurs in the region containing Ala1 and the N-terminal acetyl group (Figure 7), and omission of the C² atoms from these residues reduces the r.m.s. deviation of the two structures to 0.51 Å. This region lies at the smaller of two interfaces that profilin makes with actin in crystals of profilin- β -actin (Schutt *et al.*, 1993) and the conformational change in the actin-bound structure enables the acetyl methyl group to fit into a hydrophobic pocket formed by Phe223 and Phe266 of β -actin, while the acetyl carbonyl oxygen could participate in a hydrogen bond with Tyr188 of β -actin. This interaction would require a *cis* peptide bond connecting the N-terminal acetyl group to Ala1 which was not reported in our previous description of the structure of profilin- β -actin (Schutt *et al.*, 1993). Refinement of the structure of crystalline profilin-actin at the resolution limit of the crystals, approximately 1.8 Å (Schutt *et al.*, 1989), should confirm the presence of this *cis* peptide bond. For Ala1, (ϕ , ψ) values were (-51°, 100°) for free profilin and (88°, 75°) for profilin bound to actin, while for Gly2 the values were (79°, 3°) and (55°, -134°), respectively. Thus, formation of the putative hydrogen bond with actin would come at the expense of profilin adopting a more strained conformation for Ala1.

Less dramatic conformational differences occur at the turns containing residues 65 through 68 and 92

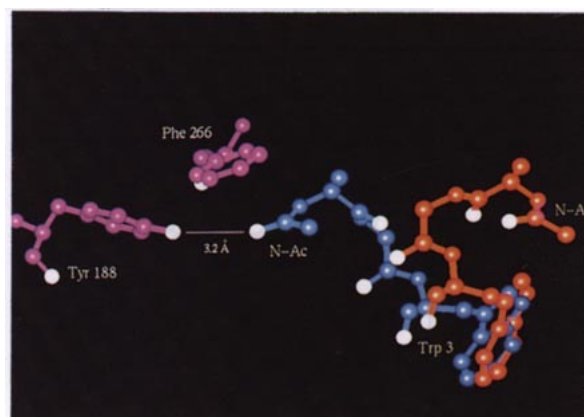


Figure 7. Conformations of the amino termini of profilin in crystals of profilin (orange) and profilin-actin (blue). For each case, the *N*-acetyl group (N-Ac) is shown along with Ala1, Gly2 and Trp3 (labeled). Oxygen atoms are white. In crystalline profilin-actin, the *N*-acetyl carbonyl group may form a hydrogen bond of approximately 3.2 Å with the phenol hydroxyl group in Tyr188 of β -actin (purple), while the *N*-acetyl methyl group could lie in proximity to the phenyl ring of Phe266. Such an interaction would require the *N*-acetyl-Ala1 peptide bond to lie in the *cis* orientation. Although not reported in the 2.55 Å structure of profilin- β -actin (Schutt *et al.*, 1993), this conformational detail should be discernible at the resolution limit of the crystals, approximately 1.8 Å (Schutt *et al.*, 1989). Figure made using INSIGHT-II (Bio-Sym, San Diego, U.S.A.).

through 95, both of which adopt type II configurations in the present 2.0 Å resolution refinement. These turns lie in a type I and a non-standard configuration, respectively, in the 2.55 Å structure of profilin bound to actin (Schutt *et al.*, 1993). Since neither turn lies at a profilin-actin interface, it is possible that these do not represent actual conformational differences between the two structures, but rather, new interpretations resulting from the improved electron density at higher resolution.

In addition to main-chain conformational differences between the two profilin structures, rotamer differences also are apparent for the side-chains of a number of residues. These differences do not represent significant reorientations of functional groups, except in several instances for which movement of side-chains on profilin is required to accommodate an interface with actin. Compared to the actin-free structure, the side-chain of Lys69 in profilin complexed to β -actin is rotated by -90° about the C ^{β} -C ^{γ} bond to allow formation of a salt bridge to Asp288 of β -actin; in contrast, adjacent Lys90, which forms a salt bridge to Asp 286 of β -actin, lies in nearly identical conformations in the two structures. Arg74 forms a salt bridge to the C-terminal carboxylate of β -actin by rotating its side-chain about the C ^{γ} -C ^{δ} bond by -90°, relative to the uncomplexed profilin structure. Lys113 of β -actin forms a salt bridge to Glu82 of profilin only after

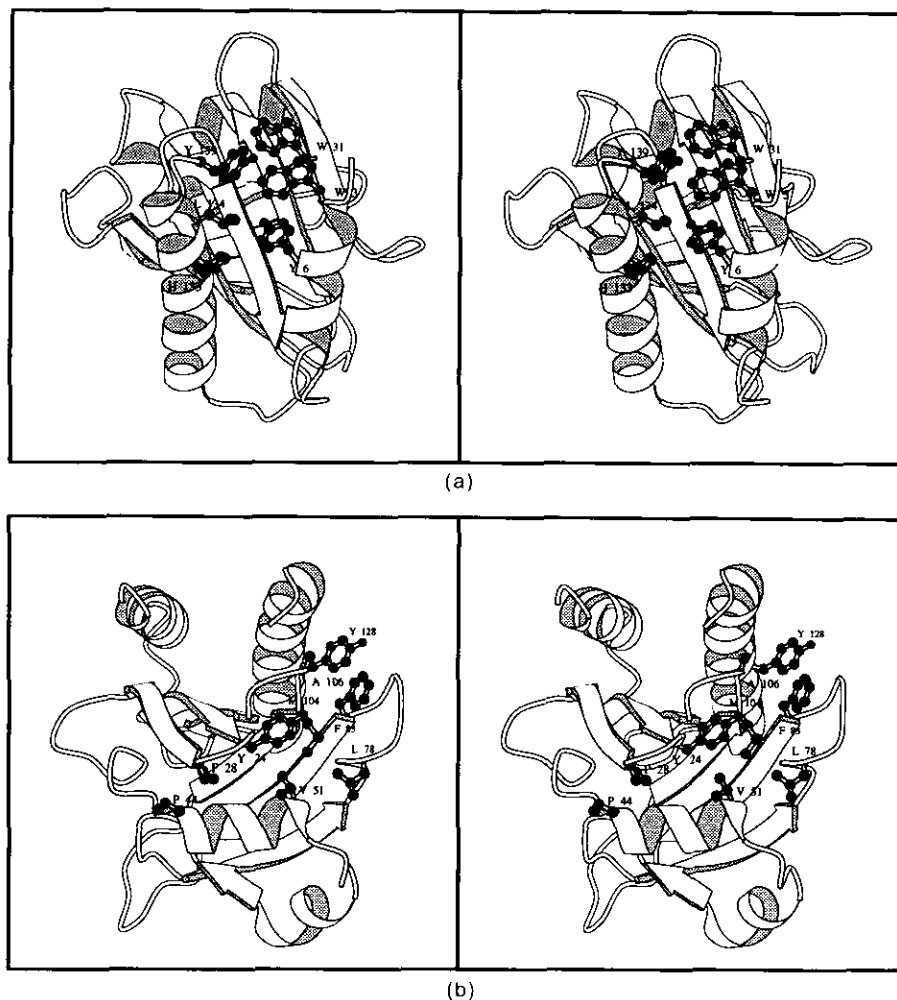


Figure 8. Solvent-exposed hydrophobic surfaces of profilin. (a) Stereo view of profilin showing the position of conserved poly(L-proline)-binding surface (Björkegren *et al.*, 1993) encompassing residues Trp3, Tyr6, Trp31, His133, His134 and Tyr139 (ball-and-stick models). Secondary structure elements of profilin are depicted by bedsprings (α -helices) and arrows (β -strands). Trp3, Tyr6 and Trp31 are invariant among all profilin isoforms, with the exception of the putative profilin from *Vaccinia virus*. (b) Different view of profilin showing the 2nd solvent-exposed hydrophobic surface of profilin composed of side-chains of residues Tyr24, Pro28, Pro44, Val51, Leu78, Phe83, Met104, Ala106 and Tyr128 (ball-and-stick models). Figure made using MOLSCRIPT (Kraulis, 1991).

movements of both the glutamate and Gln79, which otherwise would block the interaction. Finally, the 2.0 Å refinement of profilin shows a repositioning of Arg135, allowing the δ -guanido group to form a π -electron interaction with Phe83. Since neither Phe83 nor Arg136 contributes to contacts with actin or other profilin molecules in either crystal form, this difference may, as in the case of the two turns described above, be due to improved quality of data in the current refinement.

(d) Distribution of aromatic residues

The distribution of aromatic residues in profilin differs markedly from that normally observed for soluble proteins. The main hydrophobic core is composed of side-chains from residues Ala20, Val22, Val30, Ala33, Phe39, Ile42, Val47, Leu63, Leu65, Leu77, Met85, Leu87, Ile100, Val102, Leu109, Leu111 and Met113 and is unusual in that it

contains only one aromatic residue. A second, smaller, hydrophobic core is formed by side-chains associated with the packing of the N and C-terminal helices against the opposite side of the central β -pleated sheet, and incorporates no aromatic residues. In contrast, the majority of the aromatic residues in profilin lie at the surface and are accessible to solvent. These residues contribute to the relatively high proportion of non-polar surface area on profilin (59% as calculated according to Lee & Richards (1971)).

Hydrophobic residues on the surface of profilin localize to two patches, neither of which contribute to interfaces with actin (Schutt *et al.*, 1993). Trp3, Tyr6, Trp31, His133, Leu134 and Tyr139 form a predominantly aromatic patch at the interface of the N and C-terminal helices (Figure 8(a)). This patch has a solvent-exposed surface area of 284 Å² and is highly conserved among both mammalian and non-mammalian isoforms of profilin (Table 4).

Refinement at 2.0 Å establishes that the side-chains of Trp3, Tyr6, Trp31 and Tyr139 form a true aromatic cluster stabilized (Burley & Petsko, 1985) by enthalpically favorable pair-wise interactions between δ^+ hydrogen atoms and δ^- π -electron clouds of neighboring aromatic rings. The conformation of Trp31 adopts a highly strained (Schrauber, 1993) χ_2 angle of 3° in forming its aromatic-aromatic interaction with Trp3.

Solvent-exposed aromatic clusters have been observed in the antigen-binding sites of human immunoglobulin Fab fragments (Novotny & Haber, 1985), the prolyl isomerases cyclophilin (Pfügl *et al.*, 1993; Thériault *et al.*, 1993) and FKBP-12 (Van Duyn *et al.*, 1993), and the putative ligand-binding sites of Src homology 3 (SH3) domains (Musacchio *et al.*, 1992). Mutagenesis of Trp3 or His133 (Björkegren *et al.*, 1993) abolishes the specific affinity (Tanaka & Shibata, 1985) of profilin for poly(L-proline), suggesting a role for this hydrophobic surface as a binding site for proline-containing sequences (Schutt *et al.*, 1993).

A second solvent-exposed hydrophobic surface area of 410 Å² is shown in Figure 8(b) and is formed mainly from side-chains contributed by Tyr24, Pro28, Pro44, Val51, Leu78, Phe83, Met104, Ala106 and Tyr128, which lie on helix 2 and on turns 1, 6 and 8 (Table 2). This hydrophobic area is unique to mammalian profilins (Table 4). Like the first hydrophobic patch, it does not lie at an actin-binding site in crystalline profilin-actin, except for Tyr128, which forms a π -electron interaction with the δ -guanido group of Arg372 of actin.

(e) Ordered water molecules

The refined structure of free bovine profilin contains 128 crystallographically ordered water molecules, all with atomic temperature factors less than 50 Å². Water molecules are located at a large number of solvent-exposed main-chain amide nitrogen atoms and carbonyl oxygen atoms, as well as at hydrophilic side-chains, in many instances forming bridges between neighboring residues. In addition, networks of multiply bonded water molecules are found at solvent-exposed hydrophobic sites, although not at the predominantly aromatic poly(L-proline)-binding patch.

The clearest cases of structurally important water molecules in bovine profilin occur where hydrogen bonds between main-chain atoms and water molecules stabilize non-standard turns. For example, in the γ -turn connecting strands 1 and 2, the expected hydrogen bond (Baker & Hubbard, 1984) between the i and $i+2$ residues (Lys25 and Ser27, respectively) is absent, and water molecule 27 hydrogen bonds to the carbonyl oxygen atoms of Lys25 and Ser27 as shown in Figure 9(a). A second non-standard turn connects helix 1 to strand 1 and is stabilized by two centrally positioned water molecules (5 and 24) which form hydrogen bonds with carbonyl oxygen atoms of Leu10, Met11 and

Cys16, amide nitrogen atoms of Gly14 and Cys16, and one of the carboxylate oxygen atoms of Asp13. This is shown in Figure 9(b). A third non-standard turn shown in Figure 9(c) connects helix 2 with helix 3. In this case, water molecule 42 stabilizes the connecting turn by hydrogen bonding to the main-chain carbonyl oxygen atoms of Ile49 and Asp54. At the same time, water molecule 41 hydrogen bonds to the carbonyl oxygen atom of Asp54 and the amide nitrogen of Phe58, effectively substituting for the standard $i \rightarrow i+4$ hydrogen bond in this distorted α -helix.

(f) Crystal packing interactions

Bovine profilin crystallizes in the space group *C2*. A total of 107 unique atomic contacts, defined by interatomic distances of less than 4 Å ($r < 4$ Å), are made between symmetry-related molecules. These contacts include 11 hydrogen-bonding interactions, and two ion pair interactions. A noticeable feature is the packing of the conserved hydrophobic poly(L-proline)-binding patch of one profilin molecule against the loop connecting residues 90 through 96 of a symmetry-related molecule. This interaction has 43 interatomic contacts ($r < 4$ Å) including six hydrogen bonding interactions. Although Trp31 lies in this hydrophobic patch, its strained conformation (see section (b), above), is not attributable to the formation of this crystal contact, since a similar conformation found in crystalline profilin- β -actin does not use this residue in any crystal contacts.

(g) Comparison with other profilins

Mammalian profilins are highly conserved, with sequence identities exceeding 90%. The recently identified human profilin II gene (Honore *et al.*, 1993) is an exception, with only a 60% sequence identity to human profilin I. Nevertheless, residues at the two bovine profilin-actin interfaces (Schutt *et al.*, 1993) are highly conserved in human profilin II, the only difference being the substitution of a glutamate for a serine at position 56. This change could lead to the formation of an additional salt bridge between Glu56 of human profilin II and Lys284 of actin.

The polypeptide fold of bovine profilin is generally similar to that of human profilin recently solved by NMR spectroscopy (Metzler *et al.*, 1993). Secondary structural elements use almost identical amino acid residues in the two structures, which was expected since the amino acid sequences of human and bovine profilin differ by only three residues. The most apparent structural difference is that human profilin does not contain a helix between residues 56 and 61 (helix 3 in bovine profilin). This difference may be due to the distorted (ϕ, ψ) angles of this helix, which is identified as such mainly on the basis of hydrogen-bonding interactions, including the intercalated water molecule between Asp54 and Phe58 (see section (e), above).

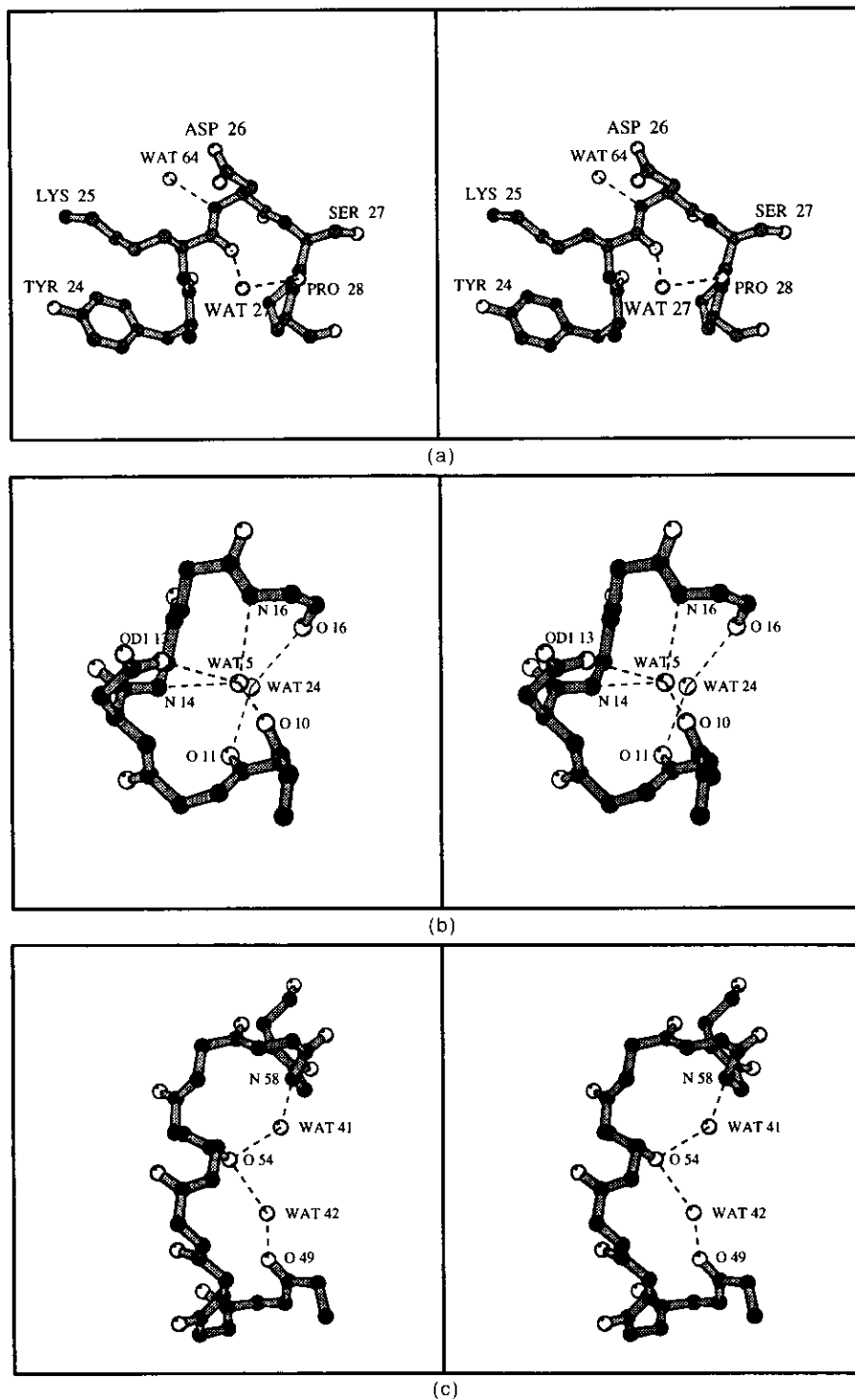


Figure 9. Role of water molecules in stabilizing non-standard elements of secondary structure. (a) γ -turn connecting strands 1 and 2. Oxygen, nitrogen, and carbon atoms are depicted as open, filled and hatched balls, respectively. Hydrogen atoms are not shown. Atoms are drawn at an atomic radius of 0.9 Å, and are therefore not to scale with bond lengths (stippled sticks). Water molecule 27 (WAT27) is hydrogen bonded (broken lines) to the carbonyl atoms of Lys25 and Ser27, substituting for the bond between the carbonyl of Lys25 and the amide nitrogen of Ser27 that would be expected in a standard γ -turn (Baker & Hubbard, 1984). Water molecule 64 hydrogen bonds to the amide nitrogen of Asp26, but does not appear to affect directly the conformation of the turn. (b) Turn connecting helix 1 to strand 1, including residues 10 to 16. Atoms are depicted as in (a), but side-chain atoms are shown only for Asp13. Water molecule 5 makes hydrogen bonds (broken lines) with the carbonyl oxygen of Leu10, amide nitrogen atoms of Gly14 and Cys16, and the carboxylate carbonyl of Asp13. Water molecule 24 hydrogen bonds to the carbonyl oxygen atoms of Met11 and Cys16. (c) Turn connecting helix 2 to helix 3, including the first turn of helix 3. Atoms are depicted as in (a) but with side-chains omitted. Water molecule 41 hydrogen bonds to the carbonyl oxygen of Asp54 and the amide nitrogen of Phe58, effectively completing the 1st hydrogen-bond interaction at the amino terminus of helix 3. Consequently, this helical turn is somewhat distorted (Table 3). Water molecule 42 hydrogen bonds to the carbonyl oxygen atoms of Ile49 and Asp54. By thus hydrogen bonding to 2 crystallographically ordered water molecules, Asp54 is a key residue in this

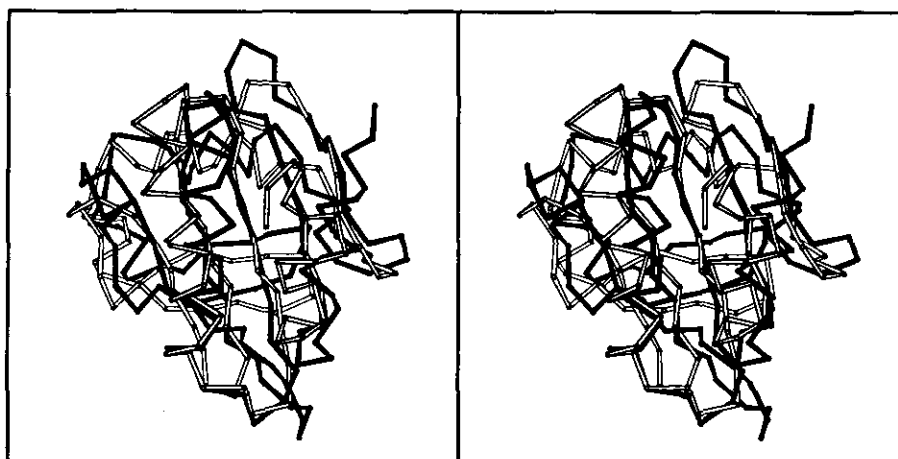


Figure 10. Comparison of the X-ray crystal structure of bovine profilin at 2.0 Å resolution with the NMR solution structure of *Acanthamoeba* profilin I (Vinson *et al.*, 1993). Connected C α atoms of bovine profilin are shown as filled sticks and those of *Acanthamoeba* profilin I (Model 1 of entry PDBPRF1.ENT in the Brookhaven Protein Data Bank) are shown as open sticks. Residues 17 to 77, 84 to 89 and 98 to 139 of bovine profilin and residues 1 to 125 of *Acanthamoeba* profilin were superimposed using protocols implemented in X-PLOR (Brünger, 1992). Figure made using MOLSCRIPT (Kraulis, 1991).

Bovine profilin is also very similar to the acidic isoform of profilin (profilin I) from *Acanthamoeba castellanii*, whose structure has been determined recently by NMR spectroscopy (Vinson *et al.*, 1993). The *Acanthamoeba* profilin structure contains almost the same secondary structural elements as bovine profilin (reviewed by Rozycki *et al.*, 1994), despite much larger differences in the amino acid sequences between the two proteins. As with the NMR structure of human profilin, the distorted helix 3 of bovine profilin is not identified in profilin from *Acanthamoeba*. Structural differences occurring at deletions in the *Acanthamoeba* sequence (Table 4) near the turns connecting strand 4 to strand 5 and strand 5 to 6 eliminate the protruding loops observed in bovine profilin, and one of these deletions appears to have a large effect on the orientation of the carboxyl-terminal helix 4. Compared to bovine profilin, the C-terminal helix in *Acanthamoeba* profilin is less tilted with respect to the orientation of strands in the central β -pleated sheet than is the case for bovine profilin. This arises from the absence of a protrusion, pushing against one side of the helix, which is formed by residues 79 to 82 in bovine profilin, and from a distortion of the N-terminal helix in *Acanthamoeba* profilin which places the amino terminus itself against the opposite side of the C-terminal helix (Figure 10). In contrast, the central β -sheets of the bovine and *Acanthamoeba* profilins superimpose well, in particular strands 1, 2, 6 and 7.

4. Discussion

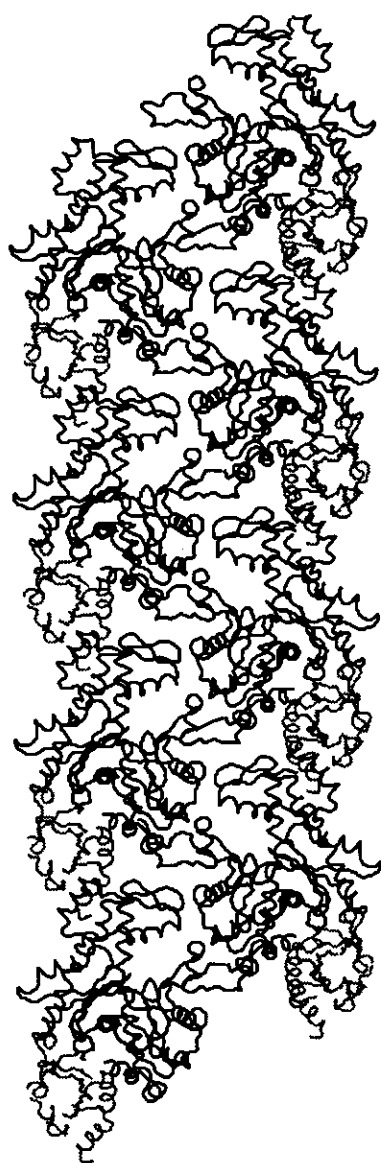
(a) Free and bound states of profilin

Refinement of bovine profilin at 2.0 Å resolution in the absence of actin allows an examination of the structural consequences for profilin in binding to

actin. Generally, the polypeptide fold of profilin does not change during the formation of profilin-actin interactions, as C α atoms from the actin-bound and actin-free structures can be superimposed with an r.m.s. positional deviation of 0.51 Å if Ala1 and the N-terminal acetyl group are omitted. The side-chains of the majority of the residues in profilin are similarly oriented in the two structures, although several exhibit significant rotamer changes in accommodating contacts with actin.

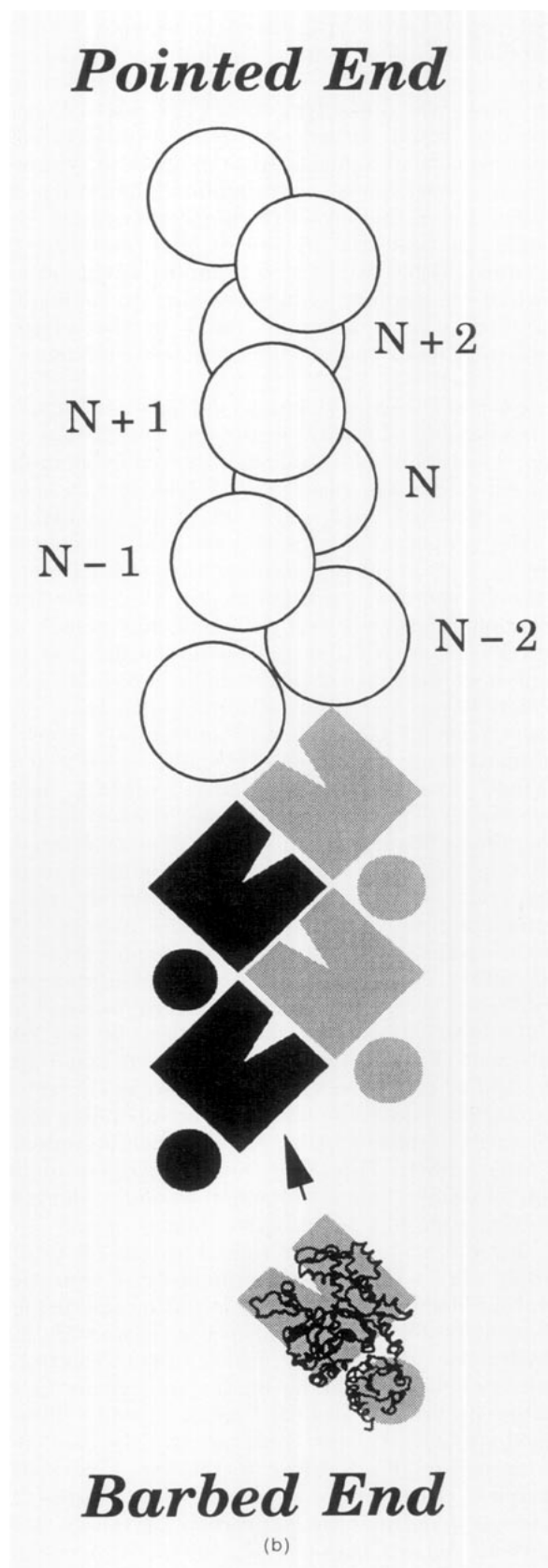
Bovine profilin makes two extensive contacts with actin molecules in crystalline profilin- β -actin (Schutt *et al.*, 1993), and this observation provides structural evidence that profilin may regulate cytoskeletal dynamics by binding oligomeric forms of actin. The specificity of profilin for poly(L-proline) (Tanaka & Shibata, 1985) opens the possibility that profilin binding to proline-containing peptides may play an additional, but still unidentified, role in controlling actin filament assembly reactions (Schutt *et al.*, 1993; Rozycki *et al.*, 1994). This notion is supported by observations (Björkegren *et al.*, 1993; Archer *et al.*, 1994; Metzler *et al.*, 1994) that the binding site for poly(L-proline) lies at a conserved patch of hydrophobic residues reminiscent of those found in other small proteins which bind proline-containing peptides, such as FKBP-12 (Van Duyne *et al.*, 1993), cyclophilin (Pfügl *et al.*, 1993; Thériault *et al.*, 1993) and SH3 domains (Musacchio *et al.*, 1992).

Ala1 and the N-terminal acetyl group lie immediately adjacent to this poly(L-proline) binding site. Together, these two residues present approximately 90 Å² of buried surface area to actin, or about 20% of the contribution of profilin to the smaller of the two profilin-actin interfaces in the profilin-actin ribbon (Schutt *et al.*, 1993). In binding to actin, they adopt a more strained conformation, possibly enabling a hydrogen bond to form between the



(a)

Figure 11. Proposed capping of actin filaments by profilin-actin ribbon segments. (a) The ribbon observed in crystals of profilin-actin. Actin molecules (continuous black line) and profilin molecules (hatched gray line) arrange about a 2₁ screw axis parallel to the length of the ribbon. Each actin molecule binds 1 ATP molecule in the crystal (Schutt *et al.*, 1993). (b) Conformational change in actin (squares → open circles) leads to a dissociation of profilin and formation of $N-2 \rightarrow N$ and $N \rightarrow N+2$ intra-strand contacts. This conformational change may be linked to ATP hydrolysis by actin (Pantaloni & Carlier, 1993). The resulting helical filament maintains a short ribbon segment at the barbed end to receive incoming actin molecules. The length shown of the ribbon segment is illustrative and should not be construed as a prediction for the approximate length of such segments in actual growing filaments.



(b)

N-acetyl carbonyl group of profilin and Tyr188 of actin (Figure 7). Interaction of a proline-containing polypeptide with Trp3, one of the residues in human profilin required for binding poly(L-proline) (Björkegren *et al.*, 1993), could influence the profilin-actin contact in one of two ways. Peptide binding could either strain the acetyl-tyrosine hydrogen bond sufficiently to allow Ala1 to revert to the unstrained conformation, initiating the disruption of the second profilin-actin contact, or it could prevent the reversion and stabilize the contact. Either way, the N terminus would act as a switch to mediate profilin binding to actin. The strained conformation of Trp31 in the adjacent poly(L-proline) binding site may also contribute to this switch.

Such a molecular switch would have ramifications for assembly of F-actin in the cell. We have argued previously that actin ribbons observed in crystalline profilin-actin are structurally related to the helical actin filament, and may convert to the filament under proper conditions (Schutt *et al.*, 1989, 1993, 1994). This argument assumes that the actin-actin ribbon contact corresponds to the *interstrand* contact formed between each actin molecule *N* and its *N*−1 and *N*+1 neighbors in the filament (the one-start helical contact). Profilin molecules intercalate between adjacent actin molecules lying along each edge of the ribbon (Figure 11(a)), blocking formation of the *N*→*N*−2 and *N*→*N*+2 *intrastrand* filament contacts (the two-start helical contacts). The transition from ribbon to helix requires a dissociation of profilin to allow formation of the two-start *intrastrand* contacts and pivoting between actin subdomains to prevent ribbon contacts from breaking during the necessary 13° twist and 8.3 Å shortening per monomer (Schutt *et al.*, 1994). This coupling of profilin dissociation with ribbon-to-helix transitions allows actin to accommodate both ribbon and helix lattices in the same filament (Figure 11(b)). Actin filaments could grow by adding profilin-actin heterodimers to the ribbon-containing end of the filament, corresponding to the filament barbed end (Pring *et al.*, 1992; Pantaloni & Carlier, 1993). Thus, the smaller actin-recognition site of profilin bound to the barbed end would guide incoming profilin-actin heterodimers.

In summary, the N-terminal switch on profilin could play a direct role in ribbon-helix transitions during filament assembly by initiating the dissociation of profilin, possibly in conjunction with ATP hydrolysis (Pantaloni & Carlier, 1993). Control of this switch through the binding of ligands to the adjacent poly(L-proline) patch could directly mediate cytoskeletal dynamics in the cell. For example, profilin localizes to the site of host actin filament assembly on *Listeria monocytogenes*, a process requiring the expression of the bacterial protein ActA (Theriot *et al.*, 1994). ActA contains several polyproline regions (Kocks *et al.*, 1992), and its binding to profilin at the poly(L-proline)-specific hydrophobic patch could set the N-terminal switch of profilin to the "actin-accepting" state. Thus,

regulate the force-producing transitions in F-actin tails on *L. monocytogenes* (Schutt *et al.*, 1993).

(b) PtdIns(4,5)P₂ binding to profilin

Several observations must be considered in identifying the binding site on profilin for micellar PtdIns(4,5)P₂. First, fluorescence quenching experiments indicate that Trp3 and Trp31 are part of the profilin-PtdIns(4,5)P₂ interface (Raghuathan *et al.*, 1992). Second, a sequence at the carboxyl terminus of bovine profilin is homologous to two PtdIns(4,5)P₂ binding sequences in gelsolin (Yu *et al.*, 1992). Third, bovine and human profilins have similar affinities for PtdIns(4,5)P₂ (Lassing & Lindberg, 1988). At the same time, the affinity of human profilin for PtdIns(4,5)P₂ is tenfold greater than that of *Acanthamoeba* profilin II, which in turn is 10 to 50-fold greater than that of *Acanthamoeba* profilin I (Machesky *et al.*, 1990). Fourth, PtdIns(4,5)P₂ destabilizes the profilin-actin complex (Lassing & Lindberg, 1985), suggesting that it binds at or near a profilin-actin contact. Last, the stoichiometry of the interaction between micellar PtdIns(4,5)P₂ and profilin is in the range of 10:1 (Lassing & Lindberg, 1985) to 5:1 (Goldschmidt-Clermont *et al.*, 1990).

The high PtdIns(4,5)P₂:profilin stoichiometry and the fluorescence quenching of Trp3 and Trp31 suggest that a relatively large surface area of profilin may form an interface with PtdIns(4,5)P₂ micelles at or near the two tryptophan residues. This would be consistent with the observation that tryptophan residues in membrane proteins often occur at lipid-water interfaces (Schiffer *et al.*, 1992) and suggests that the conserved, solvent-exposed hydrophobic patch plays a role in binding PtdIns(4,5)P₂ as well as poly(L-proline). This patch includes His133, which is part of the consensus PtdIns(4,5)P₂-binding sequence lying on the C-terminal helix proposed by Yu *et al.* (1992). Human and bovine profilin each contain three basic residues in this consensus sequence, Lys126, Arg135 and Arg136, which are not found in the *Acanthamoeba* profilins. This would explain the higher affinities of the mammalian profilins for PtdIns(4,5)P₂ relative to those in *Acanthamoeba*, but not the different affinities observed between the two *Acanthamoeba* isoforms.

A different binding site for PtdIns(4,5)P₂ has been proposed by Vinson *et al.* (1993) based on consideration of the solution structure of *Acanthamoeba* profilin I. This site, centered around Leu24, Asn51, Lys90 and Lys93 of *Acanthamoeba* profilin I, accounts for the different affinities of the two *Acanthamoeba* profilins for PtdIns(4,5)P₂ in terms of the substitutions Leu/His24 and Asn/Lys51 in *Acanthamoeba* profilin II, which would provide a more positively charged binding surface for the acidic phospholipid. However, it does not account for the higher affinity of bovine profilin for PtdIns(4,5)P₂, since the basic residue Lys90 in the two *Acanthamoeba* profilins is replaced by the

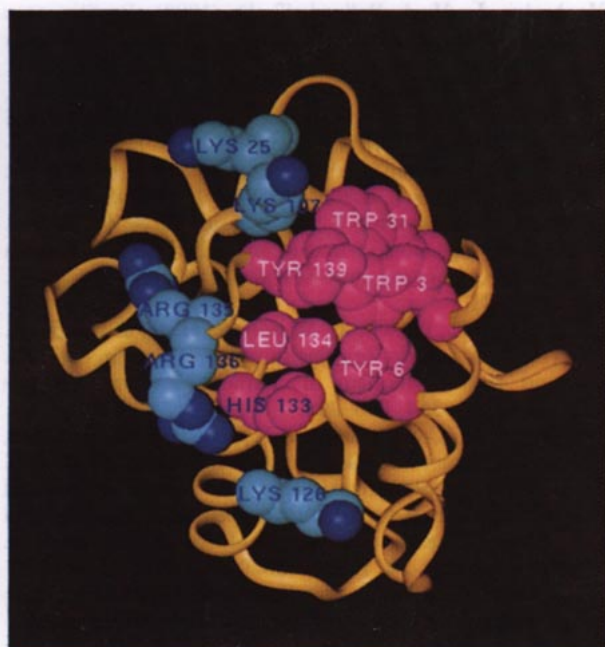


Figure 12. Proposed PtdIns(4,5)P₂ binding site of profilin. This site consists of the basic residues Lys25, Lys107, Lys126, His133, Arg135 and Arg136 (light blue, positively charged nitrogen atoms in dark blue) partially encircling the hydrophobic residues Trp3, Tyr6, Trp31, His133, His134 and Tyr139 (purple) which form the poly(L-proline) binding site. Arg 135 is partially stabilized by an amino-aromatic interaction (Burley & Petsko, 1986; Perutz *et al.*, 1986) with the aromatic ring of Phe83. Figure made using INSIGHT-II (Bio-Sym, San Diego, U.S.A).

bovine profilin. In addition, this site does not explain the fluorescence quenching of the two tryptophan residues by PtdIns(4,5)P₂.

Thus, neither proposed PtdIns(4,5)P₂-binding site can adequately explain the relative affinities of all profilin isoforms for PtdIns(4,5)P₂. However, it is noteworthy that residues 24 and 93 of *Acanthamoeba* profilin occupy positions corresponding to Lys25 and Lys107 in bovine profilin which are adjacent to the poly(L-proline)-specific hydrophobic patch containing Trp3 and Trp31. An extended PtdIns(4,5)P₂-binding site including Lys25 and Lys107, the poly(L-proline)-specific hydrophobic patch, and the consensus PtdIns(4,5)P₂-binding sequence at the carboxyl terminus (Yu *et al.*, 1992) could explain the relative affinities of the *Acanthamoeba* profilins for PtdIns(4,5)P₂ in terms of the more basic substitution Leu/His24 found in *Acanthamoeba* profilin II. This extended site is shown in Figure 12 and consists of a strongly hydrophobic center surrounded by a half-circle of positively charged side-chains.

This extended PtdIns(4,5)P₂-binding site not only accounts for the relative affinities of different profilin isoforms for PtdIns(4,5)P₂, but also the dissociation of profilin from actin in the presence of PtdIns(4,5)P₂. Interactions between residues in sub-

domain 1 of actin and the carboxyl-terminal helix of profilin could be disrupted by their proximity to the consensus sequence of Yu *et al.* (1992), which includes two residues (Lys125 and Tyr128) that interact directly with actin (Schutt *et al.*, 1993). In addition, binding of PtdIns(4,5)P₂ to profilin could disrupt aromatic interactions between Trp3, Tyr6 and Tyr139, which lie on the amino and carboxyl-terminal helices of profilin. Since both helices contribute residues to interfaces with actin, disruption of these aromatic interactions could directly affect one or both interactions with actin, especially at the N-terminal switch.

We thank J. Garbalinsky and I. Berggren for technical assistance. This work was supported by grants to C.E.S. from the National Institutes of Health (U.S.A.) and to U.L. from the Swedish Cancer Foundation, the Swedish Natural Science Research Council and the Granholms Foundation. M.D.R. was supported by a Muscular Dystrophy Association postdoctoral fellowship, and J.C.M. was supported by an N.I.H. pre-doctoral training grant in biophysics.

References

- Archer, S. J., Vinson, V. K., Pollard, T. D. & Torchia, D. A. (1994). Elucidation of the poly-L-proline binding site in *Acanthamoeba* profilin I by NMR spectroscopy. *FEBS Letters*, **337**, 145–151.
- Arndt, U. W. & Wonacott, A. J. (1977). *The Rotation Method in Crystallography*. North-Holland Publishing, Amsterdam.
- Baker, E. N. & Hubbard, R. E. (1984). Hydrogen bonding in globular proteins. *Progr. Biophys. Mol. Biol.* **44**, 97–179.
- Berridge, M. J. (1987). Inositol trisphosphate and diacylglycerol: Two interacting second messengers. *Annu. Rev. Biochem.* **56**, 159–193.
- Berridge, M. J. (1993). Inositol trisphosphate and calcium signalling. *Nature (London)*, **361**, 315–425.
- Björkegren, C., Rozycki, M. D., Schutt, C. E., Lindberg, U. & Karlsson, R. (1993). Mutagenesis of human profilin locates its poly(L-proline)-binding site to a hydrophobic patch of aromatic amino acids. *FEBS Letters*, **333**, 123–126.
- Brünger, A. T. (1990). Extension of molecular replacement: a new search strategy based on Patterson correlation refinement. *Acta Crystallogr. sect. A*, **46**, 46–57.
- Brünger, A. T. (1992). *X-PLOR (v. 3.0) Manual*. Yale University, New Haven, CT.
- Burley, S. K. & Petsko, G. A. (1985). Aromatic-aromatic interaction: a mechanism of protein structure stabilization. *Science*, **229**, 23–28.
- Burley, S. K. & Petsko, G. A. (1986). Amino-aromatic interactions in proteins. *FEBS Letters*, **203**, 139–143.
- Carrier, M.-F., Jean, C., Rieger, K. J., Lenfant, M. & Pantaloni, D. (1993). Modulation of the interaction between G-actin and thymosin β_4 by the ATP/ADP ratio: possible implication in the regulation of actin dynamics. *Proc. Nat. Acad. Sci., U.S.A.* **90**, 5034–5038.
- Carlsson, L., Nystrom, L.-E., Lindberg, U., Kannan, K., Cid-Dresdner, H., Lövgren, S. & Jörnvall, H. (1976). Crystallization of a non-muscle actin. *J. Mol. Biol.* **105**, 353–366.

- Carlsson, L., Nystrom, L.-E., Sundkvist, I., Markey, F. & Lindberg, U. (1977). Actin polymerizability is influenced by profilin, a low molecular weight protein in non-muscle cells. *J. Mol. Biol.* **115**, 465–483.
- Eichinger, L. & Schleicher, M. (1992). Characterization of actin- and lipid-binding domains in severin, a Ca^{2+} -dependent F-actin fragmenting protein. *Biochemistry*, **31**, 4779–4787.
- Engh, R. A. & Huber, R. (1991). Accurate bond and angle parameters for X-ray protein structure refinement. *Acta Crystallogr. sect. A*, **47**, 392–400.
- Finkel, T., Theriot, J. A., Dize, K. R., Tomaselli, G. F. & Goldschmidt-Clermont, P. J. (1994). Dynamic actin structures stabilized by profilin. *Proc. Nat. Acad. Sci., U.S.A.* **91**, 1510–1514.
- Goldschmidt-Clermont, P. J., Machesky, L. M., Baldassare, J. J. & Pollard, T. D. (1990). The actin-binding protein profilin binds to $\text{PtdIns}(4,5)\text{P}_2$ and inhibits its hydrolysis by phospholipase C. *Science*, **247**, 1575–1578.
- Goldschmidt-Clermont, P. J., Kim, J. W., Machesky, L. M., Rhee, S. G. & Pollard, T. D. (1991). Regulation of phospholipase C- γ 1 by profilin and tyrosine phosphorylation. *Science*, **251**, 1231–1233.
- Honore, B., Madsen, P., Andersen, A. H. & Leffers, H. (1993). Cloning and expression of a novel human profilin variant, profilin II. *FEBS Letters*, **330**, 151–155.
- Jancarik, J. & Kim, S. H. (1991). Sparse matrix sampling: a screening method for crystallization of proteins. *J. Appl. Crystallogr.* **24**, 409–411.
- Janmey, P. A. & Stossel, T. P. (1987). Modulation of gelsolin function by phosphatidylinositol 4,5-bisphosphate. *Nature (London)*, **325**, 362–364.
- Janmey, P. A., Lamb, J., Allen, P. G. & Matsudaira, P. T. (1992). Phosphoinositide-binding peptides derived from the sequences of gelsolin and villin. *J. Biol. Chem.* **267**, 11818–11823.
- Jones, T. A. (1978). A graphics model building program and refinement system for macromolecules. *J. Appl. Crystallogr.* **11**, 268–272.
- Kocks, C., Gouin, E., Tabouret, M., Berche, P., Ohayon, H. & Cossart, P. (1992). *L. monocytogenes*-induced actin assembly requires the actA gene product, a surface protein. *Cell*, **68**, 521–531.
- Kraulis, P. (1991). MOLSCRIPT: a program to produce both detailed and schematic plots of protein structures. *J. Appl. Crystallogr.* **24**, 946–950.
- Laemmli, U. K. (1970). Cleavage of structural proteins during the assembly of the head of bacteriophage T4. *Nature (London)*, **227**, 680–685.
- Lassing, I. & Lindberg, U. (1985). Specific interactions between phosphatidylinositol 4,5-bisphosphate and profilactin. *Nature (London)*, **314**, 472–474.
- Lassing, I. & Lindberg, U. (1988). Specificity of interaction between phosphatidylinositol 4,5-bisphosphate and the profilin:actin complex. *J. Cell Biochem.* **37**, 255–267.
- Lee, B. & Richards, F. M. (1971). The interpretation of protein structures: estimation of static accessibility. *J. Mol. Biol.* **55**, 379–400.
- Leslie, A. G. W., Brick, P. & Wonacott, A. J. (1986). *CCP4 Newsletter*, **18**, 33–39.
- Lindberg, U. (1966). Crystallization from calf spleen of two inhibitors of deoxyribonuclease. *J. Biol. Chem.* **241**, 1246–1248.
- Luzzati, V. (1952). Traitement statistique des erreurs dans la détermination des structures cristallines. *Acta Crystallogr. sect. A*, **5**, 802–810.
- Machesky, L. M. & Pollard, T. D. (1993). Profilin as a potential mediator of membrane-cytoskeleton communication. *Trends Cell Biol.* **3**, 381–385.
- Machesky, L. M., Goldschmidt-Clermont, P. J. & Pollard, T. D. (1990). The affinities of human platelet and *Acanthamoeba* profilin isoforms for polyphosphoinositides account for their relative abilities to inhibit phospholipase C. *Cell Regulation*, **1**, 937–950.
- Markus, M., Nakayama, T., Matsudaira, P. & Wagner, G. (1994). Solution structure of villin 14T, a domain conserved among actin-severing proteins. *Protein Sci.* **3**, 70–81.
- McLaughlin, P., Gooch, J., Mannherz, H.-G. & Weeds, A. (1993). Structure of gelsolin segment I-actin complex and the mechanism of filament severing. *Nature (London)*, **364**, 685–692.
- Metzler, W. J., Constantine, K. L., Friedrichs, M. S., Bell, A. J., Ernst, E. G., Lavoie, T. B. & Mueller, L. (1993). Characterization of the three-dimensional solution structure of human profilin: ^1H , ^{13}C , and ^{15}N NMR assignments and global folding pattern. *Biochemistry*, **32**, 13818–13829.
- Metzler, W. J., Bell, A. J., Ernst, E., Lavoie, T. B. & Mueller, L. (1994). Identification of the poly-L-proline-binding site on human profilin. *J. Biol. Chem.* **269**, 4620–4625.
- Musacchio, A., Noble, M., Pauptit, R., Wierenga, R. & Saraste, M. (1992). Crystal structure of a Src-homology 3 (SH3) domain. *Nature (London)*, **359**, 851–855.
- Nishizuka, Y. (1992). Intracellular signaling by hydrolysis of phospholipids and activation of protein kinase C. *Science*, **258**, 607–614.
- Noble, M., Musacchio, A., Saraste, M., Courtneidge, S. & Wierenga, R. (1993). Crystal structure of the SH3 domain in human Fyn; comparison of the three-dimensional structures of the SH3 domains in tyrosine kinases and spectrin. *EMBO J.* **12**, 2617–2624.
- Novotny, J. & Haber, E. (1985). Structural variants of antigen binding: comparison of immunoglobulin VL-VH and VL-VL domain dimers. *Proc. Nat. Acad. Sci., U.S.A.* **82**, 4592–4596.
- Pantaloni, D. & Carlier, M.-F. (1993). How profilin promotes actin filament assembly in the presence of thymosin β_4 . *Cell*, **75**, 1007–1014.
- Perutz, M. F., Fermi, G., Abraham, D. J., Poyart, C. & Bursaux, E. (1986). Hemoglobin as a receptor of drugs and peptides: X-ray studies of the stereochemistry of binding. *J. Amer. Chem. Soc.* **108**, 1064–1078.
- Pfögl, G., Kallen, J., Schirmer, T., Jansonius, J. N., Zurini, M. G. M. & Walkinshaw, M. D. (1993). X-ray structure of a decameric cyclophilin-cyclosporin crystal complex. *Nature (London)*, **361**, 91–94.
- Pollard, T. D. & Rimm, D. L. (1991). Analysis of cDNA clones for *Acanthamoeba* profilin-I and profilin-II shows an end to end homology with vertebrate profilins and a family of profilin genes. *Cell Motil. Cytoskel.* **20**, 169–177.
- Pring, M., Weber, A. & Bubba, M. R. (1992). Profilin-actin complexes elongate actin filaments at the barbed end. *Biochemistry*, **31**, 1827–1836.
- Raghuathan, V., Mowery, P., Rozycki, M., Lindberg, U. & Schutt, C. E. (1992). Structural changes in profilin accompany its binding to phosphatidylinositol 4,5-bisphosphate. *FEBS Letters*, **297**, 46–50.
- Richardson, J. S. & Richardson, D. C. (1989). In *Prediction of Protein Structure and the Principles of*

- Protein Conformation* (Fasman, G. D., ed.), pp. 1-98, J. D. Plenum Press, New York.
- Rozycki, M. D., Schutt, C. E. & Lindberg, U. (1991). Affinity chromatography-based purification of profilin: actin. *Methods. Enzymol.* **196**, 100-118.
- Rozycki, M. D., Myslik, J. C., Schutt, C. E. & Lindberg, U. (1994). Structural aspects of actin-binding proteins. *Curr. Opin. Cell. Biol.* **6**, 87-95.
- Safer, D., Golla, R. & Nachmias, V. T. (1990). Isolation of a 5-kilodalton actin-sequestering peptide from human blood platelets. *Proc. Nat. Acad. Sci., U.S.A.* **87**, 2536-2540.
- Schiffer, M., Chang, C.-H. & Stevens, F. J. (1992). The functions of tryptophan residues in membrane proteins. *Protein Eng.* **5**, 213-214.
- Schrauber, H. (1993). Rotamers: to be or not to be? An analysis of amino acid side-chain conformations in globular proteins. *J. Mol. Biol.* **230**, 592-612.
- Schutt, C. E., Lindberg, U., Myslik, J. C. & Strauss, N. (1989). Molecular packing in profilin:actin crystals and its implications. *J. Mol. Biol.* **209**, 735-746.
- Schutt, C. E., Myslik, J. C., Rozycki, M. D., Goonesekere, N. C. W. & Lindberg, U. (1993). The structure of crystalline profilin: β -actin. *Nature (London)*, **365**, 810-816.
- Schutt, C. E., Rozycki, M. D. & Lindberg, U. (1994). What's the matter with the ribbon? *Curr. Biol.* **4**, 185-186.
- Tanaka, M. & Shibata, H. (1985). Poly(L-proline)-binding proteins from chick embryos are a profilin and a profilactin. *Eur. J. Biochem.* **151**, 291-297.
- Theriault, Y., Logan, T. M., Meadows, R., Yu, L., Olejniczak, E. T., Holzman, T. F., Simmer, R. L. & Fesik, S. W. (1993). Solution structure of the cyclosporin A/cyclophilin complex by NMR. *Nature (London)*, **361**, 88-91.
- Theriot, J. A., Rosenblatt, J., Portnoy, D. A., Goldschmidt-Clermont, P. J. & Mitchison, T. J. (1994). Involvement of profilin in the actin-based motility of *L. monocytogenes* in cells and in cell-free extracts. *Cell*, **76**, 505-517.
- Tilney, L. G., Bonder, E. M., Coluccio, L. M. & Mooseker, M. S. (1983). Actin from *Thyone* sperm assembles on only one end of an actin filament: a behavior regulated by profilin. *J. Cell. Biol.* **97**, 112-124.
- Valenta, R., Duchene, R., Pettenburger, K., Sillaber, C., Valent, P., Bettelheim, P., Breitenbach, M., Rumpold, H., Kraft, D. & Scheiner, O. (1991). Identification of profilin as a novel pollen allergen; IgE autoreactivity in sensitized individuals. *Science*, **253**, 557-559.
- Valenta, R., Duchene, M., Ebner, C., Valent, P., Sillaber, C., Deviller, P., Ferreira, F., Tejkl, M., Edelmann, H., Kraft, D. & Scheiner, O. (1992). Profilins constitute a novel family of functional plant pan-allergens. *J. Exp. Med.* **175**, 377-385.
- Van Duyne, G. D., Standaert, R. F., Karplus, P. A., Schreiber, S. L. & Clardy, J. (1993). Atomic structures of the human immunophilin FKBP-12 complexes with FK506 and rapamycin. *J. Mol. Biol.* **229**, 105-124.
- Venkatachalam, C. M. (1968). Stereochemical criteria for polypeptides and proteins. V. Conformation of a system of three linked peptide units. *Biopolymers*, **6**, 1425-1536.
- Vinson, V. K., Archer, S. J., Lattman, E. E., Pollard, T. D. & Torchia, D. A. (1993). Three-dimensional solution structure of *Acanthamoeba* profilin-I. *J. Cell. Biol.* **122**, 1277-1283.
- Weber, A., Nachmias, V. T., Pennise, C. R., Pring, M. & Safer, D. (1992). Interaction of thymosin β_4 with muscle and platelet actin: implications for actin sequestration in resting platelets. *Biochemistry*, **31**, 6179-6185.
- Wilmot, C. M. & Thornton, J. M. (1988). Analysis and prediction of the different types of β -turn in proteins. *J. Mol. Biol.* **203**, 221-232.
- Yu, F., Sun, H., Janmey, P. A. & Yin, H. (1992). Identification of a polyphosphoinositide-binding sequence in an actin monomer-binding domain of gelsolin. *J. Biol. Chem.* **267**, 14616-14621.
- Zeppezauer, M., Eklund, H. & Zeppezauer, E. (1968). Micro-diffusion cells for the growth of single protein crystals by means of equilibrium dialysis. *Arch. Biochem. Biophys.* **126**, 564-573.

Edited by R. Huber

(Received 5 January 1994; accepted 15 April 1994)